



Glucocorticoid-induced activation of NOX/ROS/NF- κ B signaling in MSCs contributes to the development of GONFH

Huihui Xu^{1,2,3} · Qinghe Zeng^{1,2,3} · Kaiao Zou^{1,2,3} · Haipeng Huang^{1,2,3} · Jiali Chen^{1,3} · Pinger Wang^{1,3} · Wenhua Yuan^{1,3} · Luwei Xiao^{1,3} · Peijian Tong^{1,2,3} · Hongting Jin^{1,2,3}

Accepted: 27 May 2023 / Published online: 12 June 2023

© The Author(s), under exclusive licence to Springer Science+Business Media, LLC, part of Springer Nature 2023

Abstract

Background: This study aimed to investigate the pathogenic factors of glucocorticoids (GCs)-induced osteonecrosis of the femoral head (GONFH) and its underlying pathogenesis *in vivo* and *in vitro*. **Methods:** Radiographical (μ CT) scanning, histopathological, immunohistochemical, reactive oxygen species (ROS) and tunel staining were conducted on GONFH patients and rats. ROS, tunel, flow cytometry, alkaline phosphatase, Oil red O staining, reverse transcription-quantitative PCR and western blotting were applied to elucidate the exact pathogenesis mechanism. **Results:** Clinical and animal studies demonstrated increased levels of ROS, aggravated oxidative stress (OS) microenvironment, augmented apoptosis and imbalance in osteogenic/lipogenic in the GONFH group compared to the control group. The fate of mesenchymal stem cells (MSCs) directed by GCs is a crucial factor in determining GONFH. *In vitro* studies further revealed that GCs promote excessive ROS production through the expression of NOX family proteins, leading to a deterioration of the OS microenvironment in MSCs, ultimately resulting in apoptosis and imbalance in osteogenic/lipogenic differentiation. Furthermore, our results confirmed that the NOX inhibitor-diphenyleneiodonium chloride and the NF- κ B inhibitor-BAY 11-7082 ameliorated apoptosis and osteogenic/lipogenic differentiation imbalance of MSCs induced by an excess of GCs. **Conclusion:** We demonstrated for the first time that the aggravation of the OS microenvironment in MSCs caused by high doses of GCs leading to apoptosis and differentiation imbalance is a crucial factor in the pathogenesis of GONFH, mediated through activating the NOX/ROS/NF- κ B signaling pathway.

Keywords Oxidative stress · Mesenchymal stem cell · Apoptosis · Differentiation · GONFH

Introduction

Osteonecrosis of the femoral head (ONFH) is a clinically devastating and progressive disorder without effective therapy. As the most common type of non-traumatic

ONFH, glucocorticoids (GCs)-induced ONFH (GONFH) frequently occurs in patients treated with systemic GCs [1]. The World Health Organization has recommended systemic GCs as adjunctive therapy for coronavirus disease 2019 [2]. However, regarding the prevalence of GONFH (24%) in patients treated with GCs for severe acute respiratory syndrome (SARS) in 2003, [3] it is therefore predictable that the number of GONFH patients is expected to considerably increase in the near future owing to the widespread prevalence of COVID-19 and the extensive usage of GCs.

The precise pathological mechanism of GONFH has yet to be wholly proven. Nevertheless, apoptosis and imbalance in osteogenic/lipogenic differentiation of mesenchymal stem cells (MSCs) are the predominant pathological characteristics, ultimately resulting in structural alterations of the femoral head and severe damage to the hip joint [4–6]. It has been demonstrated that high doses of GCs not only lead to apoptosis of MSCs [7,8] but also shift the lineage

✉ Hongting Jin
hongtingjin@zcmu.edu.cn

Peijian Tong
peijiantongzjtc@163.com

¹ The First Affiliated Hospital of Zhejiang Chinese Medical University (Zhejiang Provincial Hospital of Chinese Medicine), Hangzhou, Zhejiang 310006, China

² The First College of Clinical Medicine, Zhejiang Chinese Medical University, Hangzhou, Zhejiang 310053, China

³ Institute of Orthopaedics and Traumatology of Zhejiang Province, Hangzhou, Zhejiang 310053, China

commitment of MSCs from the osteoblastic lineage to the adipocyte lineage, [7,9] which eventually results in an imbalance in osteogenic/lipogenic homeostasis. Hence, inhibiting apoptosis and maintaining the balance of osteogenic/lipogenic differentiation of MSCs may contribute to the prevention of GONFH at an early stage.

Numerous studies suggested that pharmacological doses of GCs triggered an exacerbation of the intracellular oxidative stress (OS) microenvironment [10–12]. The intracellular accumulation of excessive reactive oxygen species (ROS) induces elevated endoplasmic reticulum stress upon exposure to the severe OS microenvironment, eventually triggering apoptosis [13–15]. In addition, it has been demonstrated that exacerbation of the OS microenvironment alters the differentiation commitment of MSCs [16]. The above evidence provides novel insights into preventing GC-induced apoptosis and osteogenic/lipogenic differentiation destabilization in MSCs. Hence, decreasing ROS production and, thus, improving the OS microenvironment in MSCs could benefit the treatment of GONFH. In addition, several studies have shown that an excess of ROS exacerbates the OS microenvironment and activates nuclear factor-kappa B (NF- κ B), which is widely involved in inflammation, stress response, cell apoptosis and differentiation [17–19]. However, the implication of NOX/ROS/NF- κ B signaling on MSCs and bone homeostasis has not been elucidated. Whether NOX/ROS/NF- κ B signaling is altered during the pathogenesis of GONFH is unclear, and the mechanism of its action remains elusive.

In the present study, we first used clinical samples and both in vitro and in vivo experiments to induce a GONFH model to determine whether apoptosis and differentiation unbalance of MSCs due to exacerbated OS microenvironment is a crucial factor in the pathogenesis of GONFH. Secondly, we investigated the precise mechanism underlying the exacerbation of the OS microenvironment by excessive GCs in GONFH that ultimately lead to apoptosis and differentiation imbalance in MSCs.

Materials and methods

Patients

The study was approved by the Ethics Committee of the First Affiliated Hospital of Zhejiang Chinese Medical University (No. 2018-KL-005-02). Patients with advanced GONFH (ARCO stage III or IV) [20] and femoral neck fracture (FNF) were recruited at the First Affiliated Hospital of Zhejiang Chinese Medicine University from December 2018 to February 2022 and determined for total hip

replacement. Totally 20 GONFH and 15 FNF femoral head samples were collected in this study.

Cell culture and treatment

C3H10T1/2 mouse MSC lines (ATCC Manassas, VA, USA) were cultured in DMEM complemented with 10% FBS and 1% penicillin/streptomycin in a humidified incubator with 5% CO₂ at 37 °C. In specific experiments, MSCs were incubated with the NOX inhibitor (diphenyleneiodonium chloride [DPI], 10 μ M [21]) (Selleck, Shanghai, China), NF- κ B inhibitor (BAY 11-7082, 2 μ M [22]) (MedChemExpress, New Jersey, USA) before DEX administration.

CCK-8 assay

Dexamethasone (DEX; 0.01, 0.1, 1, 10 μ M; Selleck, Shanghai, China) was dosed based on a prior study [23]. In brief, MSCs (8×10^3 cells/well, 96-well plates) were cultured in a 100 μ L medium containing various concentrations of DEX. To investigate the proliferation activity of MSCs, wells cultured at different concentrations of DEX were added with 10 μ L of CCK-8 solution (Beyotime, Shanghai, China) and cultured for 2 h. OD values were acquired by recording absorbance at 450 nm using a microplate reader (Synergy H1, Vermont, USA).

Osteogenic differentiation assay

MSCs were cultured at 4×10^4 cells/well in 24-well plates. When the MSCs reached 70–80% confluence, they were induced in the osteoblast induction medium (DMEM complemented with 10% FBS, 50 μ g/ml ascorbic acid and 10 mM β -glycerophosphate) for 14 days.

Adipogenic differentiation assay

MSCs were cultured in 12-well plates at 1×10^5 cells/well. When MSCs reached 70–80% confluence, they were induced in the adipocyte-inducing medium (DMEM complemented with 10% FBS, 1 M DEX, 100 M indomethacin, 10 g/ml insulin and 0.5 mM methyl isobutyl xanthine) for 2 days. MSCs were then cultured in the adipocyte maintenance medium (DMEM complemented with 10% FBS and 10 μ g/ml insulin) for 12 days.

Intracellular ROS assay

The fluorescent dye 2',7'-dichlorofluorescein diacetate (DCFH-DA; BB-470,516; BestBio, Shanghai, China) was employed to evaluate ROS levels. Briefly, after drug intervention, MSCs cultured on glass coverslips were cultured in

the serum-free medium with 10 μ M DCFH-DA for 40 min at room temperature without light.

Tunel and annexin V-FITC/PI assays

The level of apoptosis of MSCs was assessed with the Tunel Assay Kit (C1088, Beyotime, Shanghai, China) and the Annexin V-FITC/PI kit (FXP018, 4 A Biotech Co., Ltd, Beijing, China). In brief, after drug intervention, MSCs cultured on 6-well plates were fixed in 4% paraformaldehyde for 45 min and subsequently cultured for 20 min with 0.3% Triton X. The MSCs were then cultured in tunel assay solution at 37 °C for 45 min, following incubation with DAPI for 5 min. As for Annexin V-FITC/PI, after drug intervention, MSCs cultured in 6-well plates were harvested and resuspended in 100 μ L of 1 \times binding buffer with 5 μ L Annexin V-FITC and 5 μ L PI and cultured for 5 min.

Western blotting

MSCs lysates were acquired using a modified radioimmunoprecipitation assay (RIPA) lysis buffer containing 1 mM phenylmethylsulfonyl fluoride and protease inhibitor cocktail (Cell Signaling Technology, Boston, USA). And then, proteins were quantitated by BCA Protein Assay Kit (Thermo Scientific, Waltham, USA), fractionated via sodium dodecyl sulfate-polyacrylamide gel electrophoresis gel and transferred to polyvinylidene difluoride membranes. After incubation with a solution consisting of 5% skimmed milk for 1 h at 4 °C, the polyvinylidene fluoride membrane was then incubated overnight at 4 °C with primary antibodies against nicotinamide adenine dinucleotide phosphate oxidase-2 (NOX2; dilution 1:1 000, 19013-1-AP; Proteintech, Chicago, USA), nicotinamide adenine dinucleotide phosphate oxidase-4 (NOX4; dilution 1. 1,000, ET1607-4; Huabio, Hangzhou, Zhejiang, China), caspase-3 (CASP3; dilution 1: 1,000, 9665; Cell Signaling Technology, Boston, USA), osterix (OSX; dilution 1. 1,000, ER1914-47; Huabio, Hangzhou, Zhejiang, China), peroxisome activated receptor γ (PPAR γ ; dilution 1: 1 000, AB19481; Abcam,

Cambridge, UK), and glyceraldehyde-3-phosphate dehydrogenase (GAPDH; dilution 1: 5 000, ARG10112; Arigo, Taiwan, China). The membranes were then incubated with the corresponding secondary antibodies for 2 h at 4 °C. Protein expression was then determined using an LI-COR Odyssey® scanner (LI-COR Biosciences, Nebraska, USA).

Reverse transcription-quantitative PCR (RT-qPCR)

Total RNA was harvested utilising TRIzol® reagents (Invitrogen, Carlsbad, California, USA) and cDNA was synthesized by PrimeScript™ RT kits (Takara, Beijing, China). Following the manufacturer's instructions, RT-qPCR was conducted by SYBR Premix EX Taq™ kits (Takara, Beijing, China). Primer sequences for NOX2, NOX4, CASP3, OSX, PPAR γ and β -actin are presented in Table 1.

Animal studies

All animal experiments in the present study were permitted by the Ethics Committee of Zhejiang Chinese Medical University (No. 20190401-10) and conducted according to the NIH Guide for the Care and Use of Laboratory Animals. Twelve 12-week-old male Sprague-Dawley (SD) rats (weight: 450 \pm 50 g) were obtained from SLAC Laboratory Animals, Shanghai, China Ltd (No. SCXK (Hu) 2017- 0005). The GONFH model was performed using lipopolysaccharide (LPS; Sigma-Aldrich, St. Louis, USA) combined with methylprednisolone (MPS; Pfizer, NY, USA), as described previously [24,25]. Rats were randomised into control and GONFH groups, 6 rats per group, and placed in a room at 22 \pm 3 °C and 55–60% humidity and supplied with pure water and a standard diet.

Biomechanical assay

Fresh specimens of rat femoral heads were taken and statically loaded at 0.5 mm/min with an axial compression testing machine (EnduraTec TestBench™ system, Bose Corp., Minnetonka, MN, USA). The occurrence of the first turning point of the machinery will be defined as the load-bearing ability.

Micro-CT (μ CT) assay

Femoral head specimens were acquired for μ CT (Skyscan 1176, Bruker μ CT, Kontich, Belgium) analysis with a resolution of 11 μ m to examine the bone microstructure of the femoral head. Bone mineral density (BMD), trabecular number (Tb. N), trabecular volume fraction (BV/TV) and trabecular separation (Tb. Sp) were also measured.

Table 1 Primer sequences for RT-qPCR.

Primer name	Sequence
NOX2 forward	5'-TGTGGTTGGGGCTGAATGTC-3'
NOX2 reverse	5'-CTGAGAAAGGAGAGCAGATTTTCG-3'
NOX4 forward	5'-GAAGGGGTAAACACCTCTGC-3'
NOX4 reverse	5'-ATGCTCTGCTTAAACACAATCCT-3'
CASP3 forward	5'-GTGGAGGCCGACTTCTTGATGC-3'
CASP3 reverse	5'-TGGCACAAAGCGACTGGATGAAC-3'
OSX forward	5'-CCCTTCTCAAGCACCAATGG-3'
OSX reverse	5'-AAGGGTGGGTAGTCATTTGCATA-3'
RRAR γ forward	5'-CTTGACAGGAAAGACAACGG-3'
RRAR γ reverse	5'-GCTTCTACGGATCGAAACTG-3'
β -actin forward	5'-GGAGATTACTGCCCTGGCTCCTA-3'
β -actin reverse	5'-GACTCATCGTACTCCTGCTTGTCTG-3'

Histology and histomorphometry

Femoral head samples were decalcified, embedded in paraffin and sectioned to 3 μm , then stained with Algae Blue Hematoxylin/Orange G (ABH/OG) and histologically analysed. The area of adipocytes and trabeculae, and the ratio of empty bone lacunae in the subchondral bone of the femoral head were evaluated.

ROS assay

Freshly isolated femoral head tissue was rapidly frozen and sectioned at an optimized cutting temperature at a thickness of 8 μm . ROS levels were determined using the DHE-ROS Assay Kit (BB-470,516; BestBio, Shanghai, China). In brief, slices were incubated in darkness with dihydroethidium for 40 min, followed by DAPI for 5 min.

TUNEL assay

The TUNEL Assay Kit (C1088, Beyotime, Shanghai, China) was applied to assess apoptosis in femoral head samples. Briefly, sections were dewaxed, rehydrated, and incubated in TUNEL assay solution at 37 °C for 30 min, then incubated with DAPI for 5 min.

Immunohistochemistry (IHC)

Sections were dewaxed and rehydrated, then incubated in citrate buffer for 4 h at 60 °C for antigen retrieval. Subsequently, sections were incubated with anti-RUNX2 (dilution 1:200, AB236639; Abcam, Cambridge, UK), anti-OSX (dilution 1:200, ER1914-47; Huabio, Hangzhou, Zhejiang, China), anti-PPAR γ (dilution 1:300, AB19481; Abcam, Cambridge, UK), anti-fatty acid binding protein-4 (FABP4, dilution 1:300, AB92501; Abcam, Cambridge, UK), anti-NOX2 (dilution 1:500, 19013-1-AP; Proteintech, Chicago, USA), anti-NOX4 (dilution 1:100, ET1607-4; Huabio, Hangzhou, Zhejiang, China), phosphorylated-p65 (p-p65; dilution 1:300, Arigo, ARG51518; Taiwan, China) primary antibodies, and incubated for 8 h at 4 °C in the absence of light. On day 2, sections were stained in diaminobenzidine solution in reaction with a secondary antibody (dilution 1:1000, 31,234; Invitrogen, Carlsbad, California, USA) for 30 min while counterstained with hematoxylin.

Statistical analysis

Data are shown as mean \pm SD. One-way ANOVA followed by Dunnett's test was conducted using SPSS 24.0 software. $P < 0.05$ was statistically significant, with $*P < 0.05$,

$**P < 0.01$, and $**P < 0.001$. All experiments included at least three replicates.

Results

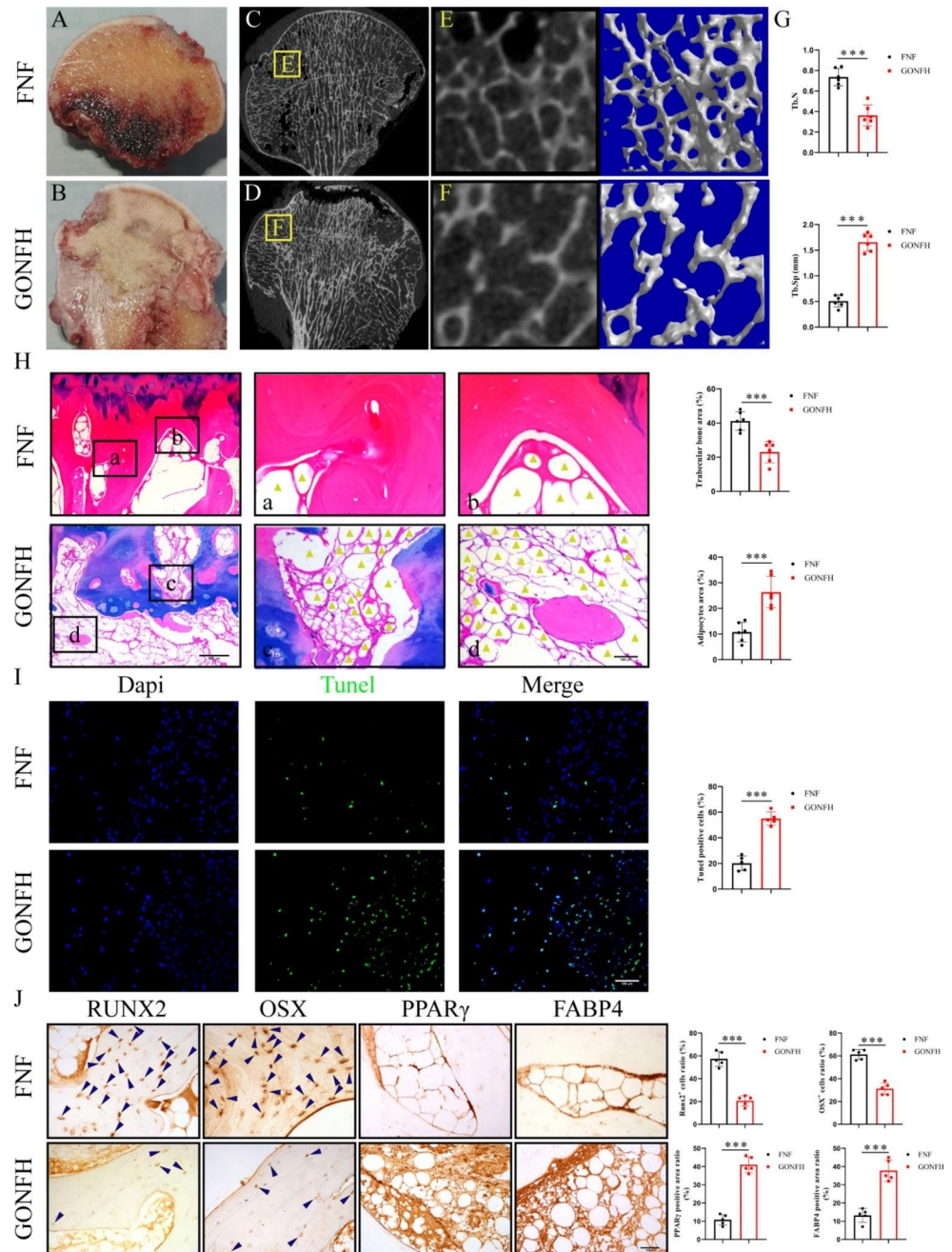
Increased apoptosis and osteogenic/lipogenic formation imbalance in the femoral head of GONFH patients

Figure 1B displayed the characteristic features of GONFH, particularly the presence of cystic alterations and large areas of collapse and necrosis of the subchondral bone in comparison with FNF (Fig. 1A). μCT images revealed the destruction of the femoral head and partial fracture of the trabeculae of the subchondral bone in GONFH compared to FNF, with a significantly reduced number of trabeculae (Fig. 1C–F). Morphological analysis of the μCT indicated that Tb.N was enhanced in GONFH than in FNF, while Tb.Sp was conversely lower (Fig. 2G). Further histopathological features were observed using ABH/OG staining, which demonstrated significantly fewer trabeculae in the subchondral bone and numerous fat vacuoles in GONFH compared to FNF (Fig. 1H). Moreover, the results of TUNEL staining displayed markedly higher levels of apoptosis in the subchondral bone of GONFH than in FNF (Fig. 1I). Furthermore, the IHC staining results indicated a marked decrease in the expression of osteogenic-associated proteins (RUNX2 and OSX) and a marked increase in the expression of lipogenic-associated proteins (PPAR γ and FABP4) in GONFH compared with FNF (Fig. 1J). These findings suggested that GONFH patients had reduced bone mass, enhanced apoptosis and imbalance in osteogenic/lipogenic formation in the femoral head.

Elevated apoptosis levels and accompanying imbalance in osteogenic/lipogenic homeostasis in the femoral head of GONFH rats

We sought to validate further the phenotype observed on clinical samples by simulating the early stages of GONFH through *in vivo* experiments. The procedure for animal experiments is shown in Fig. 2A. The femoral head in the control group was smooth, transparent and white, whereas the femoral head was unsmooth and had a dark red appearance in the GONFH group (Fig. 2B). Biomechanical tests showed a significant reduction in the load-bearing capacity in the GONFH group in comparison with the control group (Fig. 2C). Moreover, μCT images showed sparse and thinning trabeculae in the subchondral bone of the GONFH group in comparison with the control group (Fig. 2D). μCT analysis further confirmed the alterations in the bone

Fig. 1 Decreased bone mass, enhanced apoptosis and imbalance in osteogenic/lipogenic homeostasis in the femoral head of GONFH patients. **(A, B)** Gross morphology of the femoral head. **(C–F)** 2D and 3D μ CT images and quantitative analysis of the femoral head. **(G)** ABH/OG staining images and histomorphometric analysis of the femoral head. The adipocytes are indicated by yellow triangles. **(H)** TUNEL staining and quantitative analysis of the femoral head. **(I)** Immunohistochemistry staining and quantitative analysis of RUNX2, OSX, PPAR γ and FABP4 in the femoral head. The RUNX2 and OSX positive cells are indicated by blue arrows. $***P < 0.001$ (vs. GONFH).



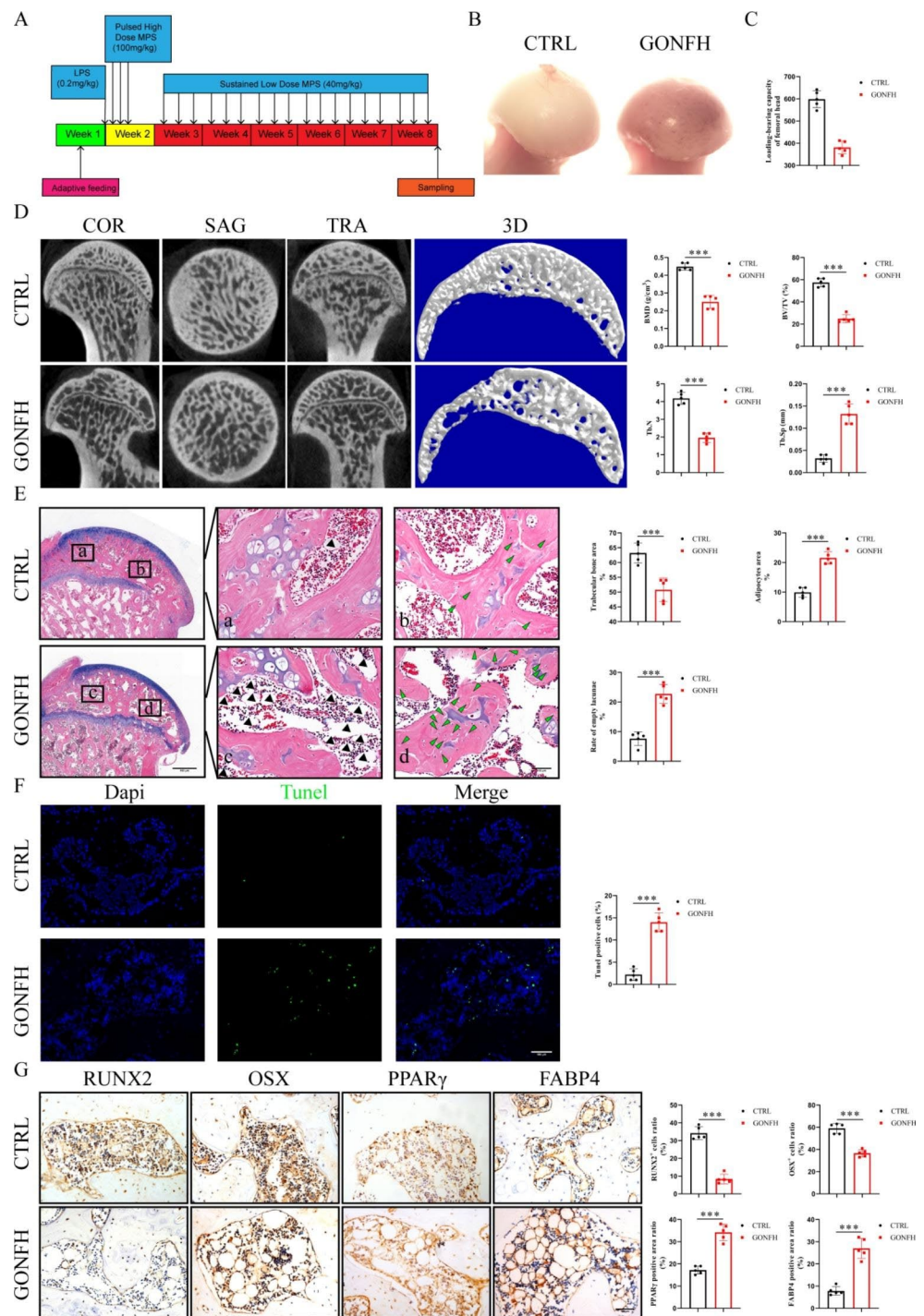
microstructure of the subchondral bone of the GONFH group, as evidenced by markedly reduced BMD, BV/TV and Tb.N, and notably elevated Tb.Sp (Fig. 2D). In addition, ABH/OG staining revealed a distinct reduction in bone volume in the subchondral bone of the GONFH group, with extensive empty bone lacunae and abundant fat in the medullary cavity (Fig. 2E). In addition, TUNEL and IHC staining results revealed that similar to the results of clinical samples, the GONFH group showed distinctly increased levels of apoptosis and lipogenesis-related protein expressions and remarkably diminished levels of osteogenesis-related protein expressions in the subchondral bone (Fig. 2F, G). These

results demonstrated that the apoptosis level was markedly elevated and accompanied by an imbalance in osteogenic/lipogenic homeostasis in the femoral head of GONFH rats.

Enhanced apoptosis and imbalance in osteogenic/lipogenic differentiation of MSCs caused by DEX

Regarding in vitro experiments, we subjected MSCs to DMEM containing different concentrations of DEX to verify whether DEX could inhibit the survival ability of MSCs. It was found that high doses of DEX ($\geq 1 \mu\text{M}$) were toxic to MSCs (Fig. 3A). We then mimicked GONFH with a $1 \mu\text{M}$

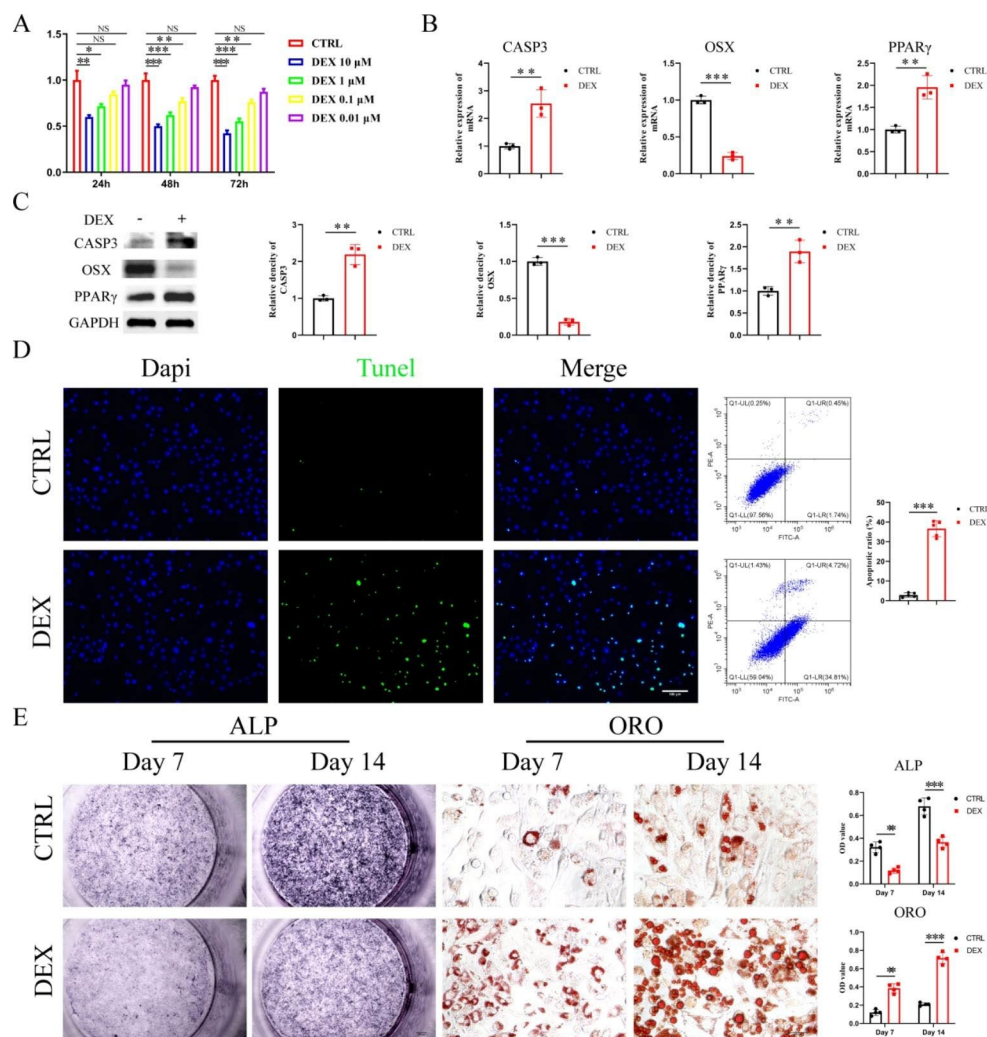
Fig. 2 Gross morphology, radiographs and histopathological images of rat femoral head samples. **(A)** The Schematic diagram of the in vivo modeling procedure. **(B)** Gross morphology of the femoral head. **(C)** The load-bearing capacity of the femoral head. **(D)** 2D and 3D μ CT images and quantitative analysis of the femoral head. **(E)** ABH/OG staining images and histomorphometric analysis of the femoral head. The adipocytes are indicated by black triangles and the empty lacunae are indicated by green arrows. **(F)** TUNEL staining images and quantitative analysis of the femoral head. **(G)** Immunohistochemistry staining and quantitative analysis of RUNX2, OSX, PPAR γ and FABP4 in the femoral head. *** $P < 0.001$ (vs. GONFH).



concentration of DEX. We found that consistent with the results from human and rat samples, a 1 μ M concentration of DEX remarkably increased the gene and protein expression levels of CASP3 and PPAR γ and diminished the expression level of OSX (Fig. 3B, C). Moreover, tunnel staining and flow cytometry results revealed that the apoptosis level was considerably lower in the DEX-treated MSCs in comparison with the control group (Fig. 3D). Additionally, ALP and Oil Red O staining results indicated that DEX treatment caused

an osteogenic/lipogenic differentiation imbalance in MSCs (Fig. 3E). The above evidence demonstrated that DEX contributed to increased apoptosis and osteogenic/lipogenic differentiation imbalance in MSCs.

Fig. 3 DEX leads to increased apoptosis and imbalance in osteogenic/lipogenic differentiation of MSCs. (A) CCK8 assay of the proliferation capacity of MSCs treated with different concentrations of 1 μ M DEX. (B) CASP3, OSX and PPAR γ mRNA of MSCs treated with DEX. (C) CASP3, OSX and PPAR γ protein levels of MSCs treated with 1 μ M DEX. (D) TUNEL staining and flow cytometry of MSCs treated with 1 μ M DEX. (E) ALP and Oil red O staining of MSCs incubated with 1 μ M DEX for 7 or 14 days. NS, no significance, ** $P < 0.01$, *** $P < 0.001$ (vs. CTRL or 1 μ M DEX).



Elevated NOX protein expressions and ROS levels in the necrotic zone of GONFH lead to the exacerbation of the OS microenvironment

Worsening of the OS microenvironment caused by elevated ROS levels has been suggested as a possible factor in the pathogenesis of GONFH, [26,27] but the exact mechanism remains to be elucidated. We then conducted validation in human and rat samples as well as in MSCs. ROS staining of human samples revealed markedly higher levels of ROS in the subchondral bone of GONFH patients compared to FNF patients (Fig. 4A). As expected, ROS levels were considerably increased in the subchondral bone of GONFH rats (Fig. 4B). Moreover, cellular experiments obtained similar results, as evidenced by remarkably enhanced ROS levels in MSCs after DEX treatment (Fig. 4C). The NOX family is essential to ROS in bone and cells, with NOX2 and NOX4 proteins being the most prominent [28–30]. Therefore, we validated the results in GONFH samples and, surprisingly, the results of clinical samples, animal samples and in vitro

cellular assays all demonstrated dramatically elevated levels of NOX2 and NOX4 gene and protein expressions in comparison with the control group. The above data revealed that NOX protein expression and ROS levels in the necrotic zone of GONFH were increased, causing an aggravation of the OS microenvironment.

DPI reversed apoptosis and imbalance in osteogenic/lipogenic differentiation of MSCs caused by NOX/ROS signaling activation

Given the above experimental results, we hypothesized that NOX/ROS signaling activation leading to apoptosis and imbalance of osteogenic/lipogenic differentiation of MSCs might be the potential pathogenesis of GONFH. Accordingly, we employed a NOX inhibitor-DPI and identified that DPI markedly inhibited the elevated levels of ROS and the gene and protein levels of NOX2 and NOX4 in MSCs caused by excessive DEX (Fig. 5A-C). Subsequently, we evaluated the efficacy of DPI on DEX-induced apoptosis and

Fig. 4 GCs-induced exacerbation of the OS microenvironment in the necrotic region of GONFH, with enhanced NOX protein expressions and ROS levels. **(A)** ROS staining and quantitative analysis of human femoral head. **(B)** ROS staining and quantitative analysis of rat femoral head. **(C)** ROS staining and quantitative analysis of MSCs treated with 1 μ M DEX. **(D)** Immunohistochemistry staining and quantitative analysis of NOX2 and NOX4 of human femoral head. **(E)** Immunohistochemistry staining and quantitative analysis of NOX2 and NOX4 of rat femoral head. **(F)** NOX2 and NOX4 mRNA of MSCs treated with 1 μ M DEX. **(G)** NOX2 and NOX4 protein levels of MSCs treated with 1 μ M DEX. PC, positive control, *** P < 0.001 (vs. GONFH or DEX).

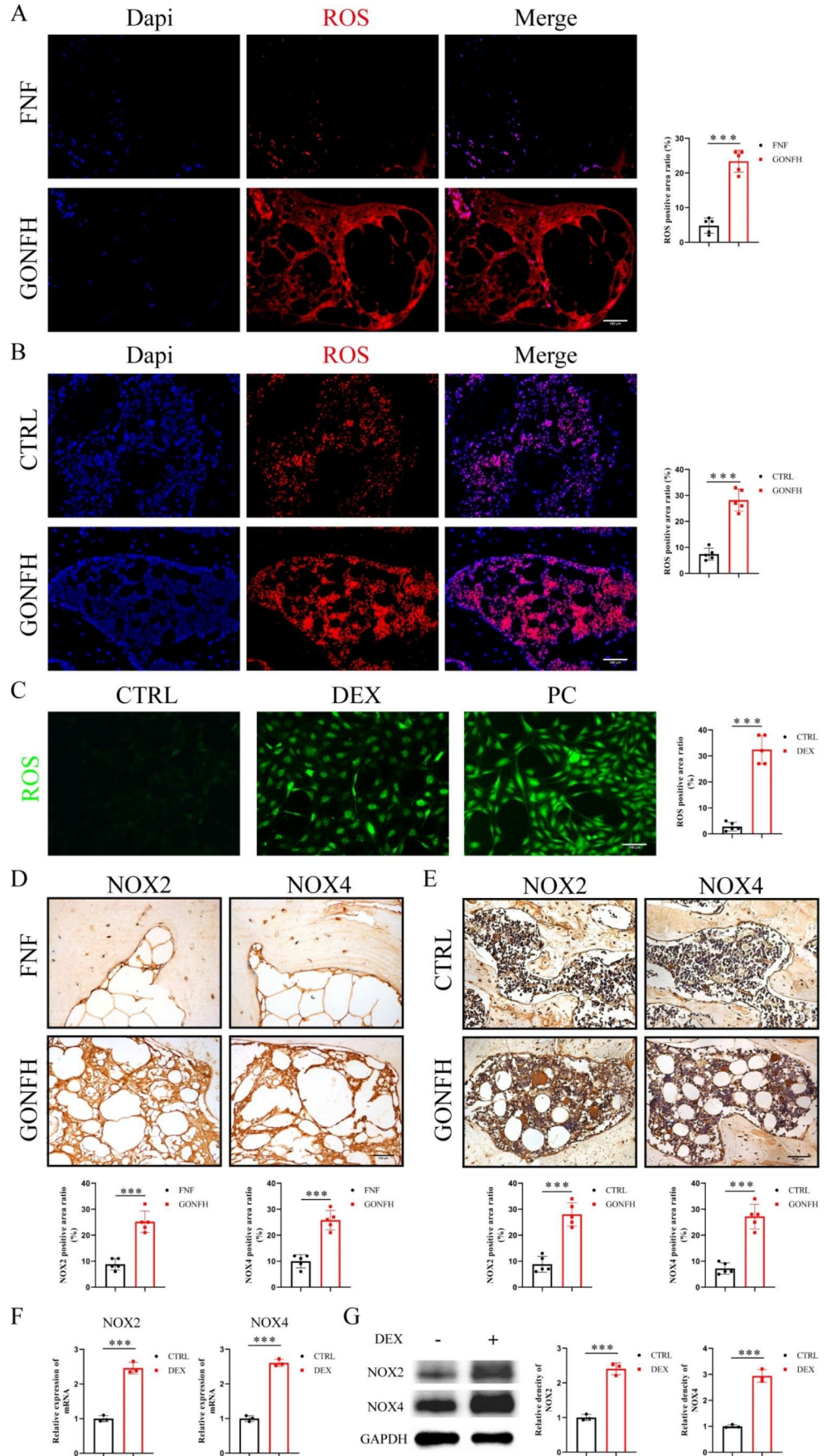
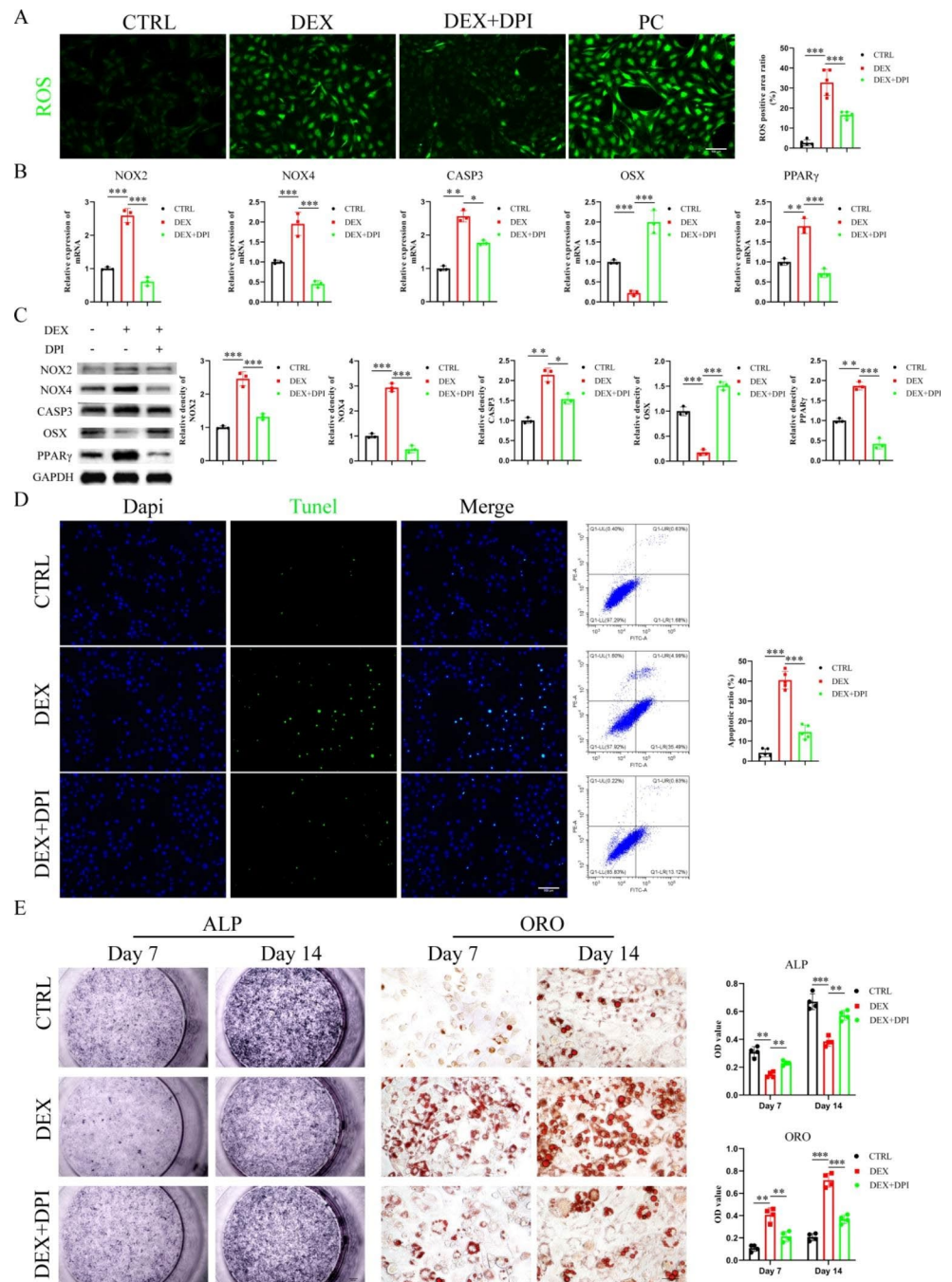


Fig. 5 DPI counteracted the OS-promoting effects of DEX and reversed apoptosis and imbalance in osteogenic/lipogenic differentiation of MSCs. **(A)** ROS staining and quantitative analysis of MSCs treated with DEX and DPI. **(B)** NOX2, NOX4, CASP3, OSX and PPAR γ mRNA of MSCs treated with DEX and DPI. **(C)** NOX2, NOX4, CASP3, OSX and PPAR γ protein levels of MSCs treated with DEX and DPI. **(D)** TUNEL staining and flow cytometry of MSCs treated with DEX and DPI. **(E)** ALP and Oil red O staining of MSCs treated with DEX and DPI for 7 or 14 days. PC, positive control. * $P < 0.05$, ** $P < 0.01$, *** $P < 0.001$ (vs. DEX).



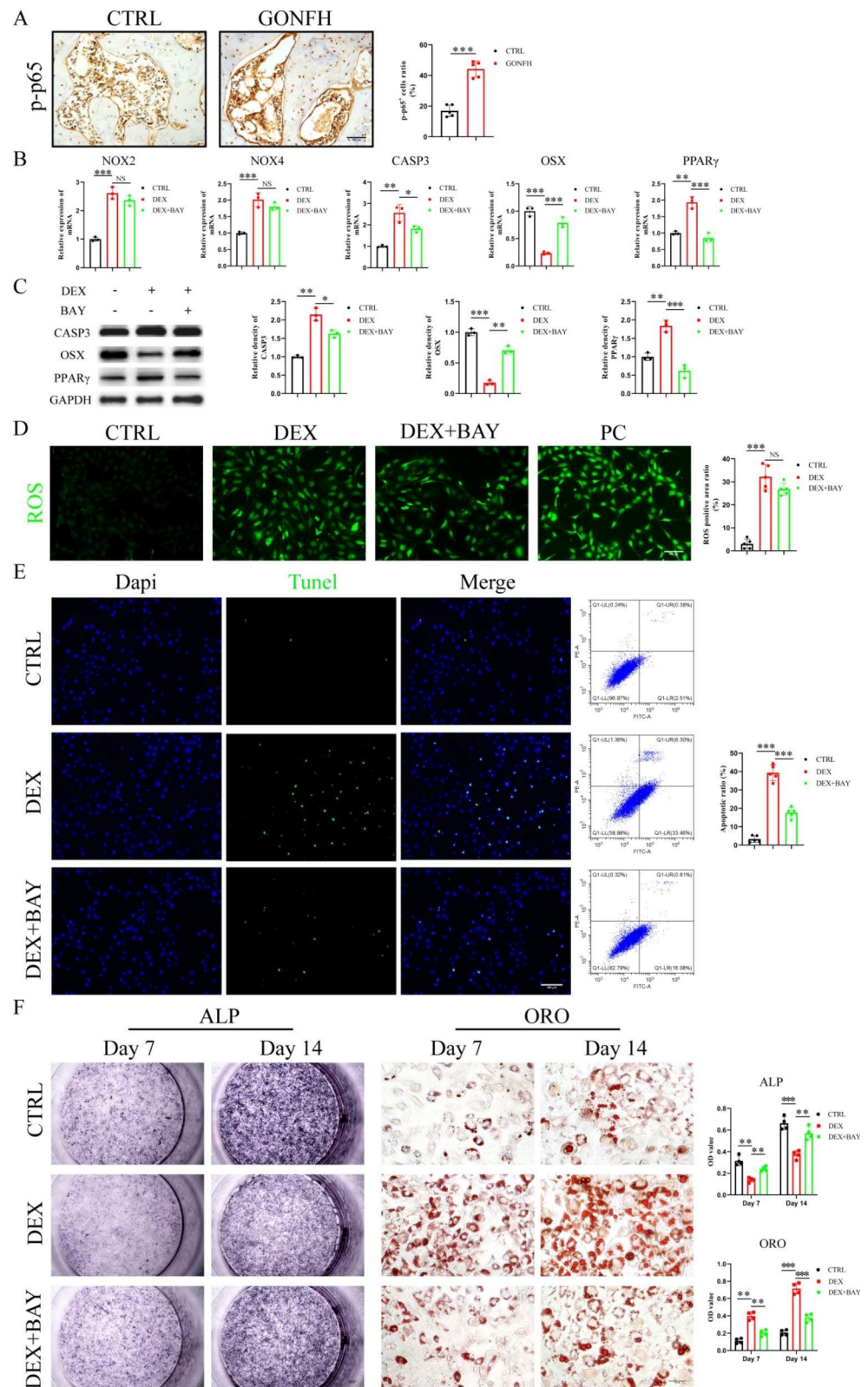
osteogenic/lipogenic differentiation in MSCs. Surprisingly, RT-qPCR and WB results demonstrated that DEX-induced over-expression of CASP3 and PPAR γ was distinctly diminished by DPI treatment. In contrast, the suppression of OSX was significantly neutralized by the addition of DPI (Fig. 5B, C). Moreover, tunel staining and flow cytometry results further confirmed that DPI treatment notably reduced the level of apoptosis in MSCs (Fig. 5D). Furthermore, ALP and Oil Red O assays also demonstrated that DPI predominantly reverted the imbalance in osteogenic/lipogenic differentiation of MSCs resulting from DEX therapy (Fig. 5E).

These results confirmed that DPI reversed apoptosis and imbalance of osteogenic/lipogenic differentiation of MSCs induced by the activation of NOX/ROS signaling.

Excess GCs caused apoptosis and destabilization of osteogenic/lipogenic differentiation in MSCs through activation of the NOX/ROS/NF- κ B signaling pathway

We performed further experiments to clarify the precise mechanism by which DEX causes apoptosis and

Fig. 6 BAY partially reversed DEX-induced apoptosis and imbalance of osteogenic/lipogenic differentiation of MSCs. **(A)** Immunohistochemistry staining and quantitative analysis of p-p65 of rat femoral head. **(B)** NOX2, NOX4, CASP3, OSX and PPAR γ mRNA of MSCs treated with DEX and BAY 11-7082. **(C)** CASP3, OSX and PPAR γ protein levels of MSCs treated with DEX and BAY 11-7082. **(D)** ROS staining and quantitative analysis of MSCs treated with DEX and BAY 11-7082. **(E)** TUNEL staining and flow cytometry of MSCs treated with DEX and BAY 11-7082. **(F)** ALP and Oil red O staining of MSCs treated with DEX and BAY 11-7082 for 7 or 14 days. PC, positive control, NS, no significance, * $P < 0.05$, ** $P < 0.01$, *** $P < 0.001$ (vs. GONFH or DEX).



differentiation imbalance in MSCs. Excess ROS has been demonstrated to activate NF- κ B signaling, which is extensively implicated in inflammation, stress responses, apoptosis

and differentiation [17–19]. Therefore, we first validated the levels of p-p65, a crucial factor in activating NF- κ B signaling, in GONFH rats. Surprisingly, the expression level of

p-p65 was considerably higher in GONFH rats (Fig. 6A). We then used BAY 11-7082, an inhibitor of NF- κ B activation, for further mechanistic studies. Both RT-qPCR and WB results showed that DEX-induced increases in CASP3 and PPAR γ expression and reduction in OSX expression were partially restored by BAY 11-7082 treatment (Fig. 6B, C). Nevertheless, the application of BAY 11-7082 failed to recover the elevated NOX2 and NOX4 expression and ROS levels induced by the DEX treatment (Fig. 6B, D). TUNEL staining, flow cytometry, ALP staining and Oil Red O staining further confirmed that BAY 11-7082 reversed apoptosis and the balance of osteogenic/lipogenic differentiation of MSCs (Fig. 6E, F). Overall, our data suggested that BAY could partially reverse the OS-induced apoptosis and the imbalance in osteogenic/lipogenic differentiation of MSCs.

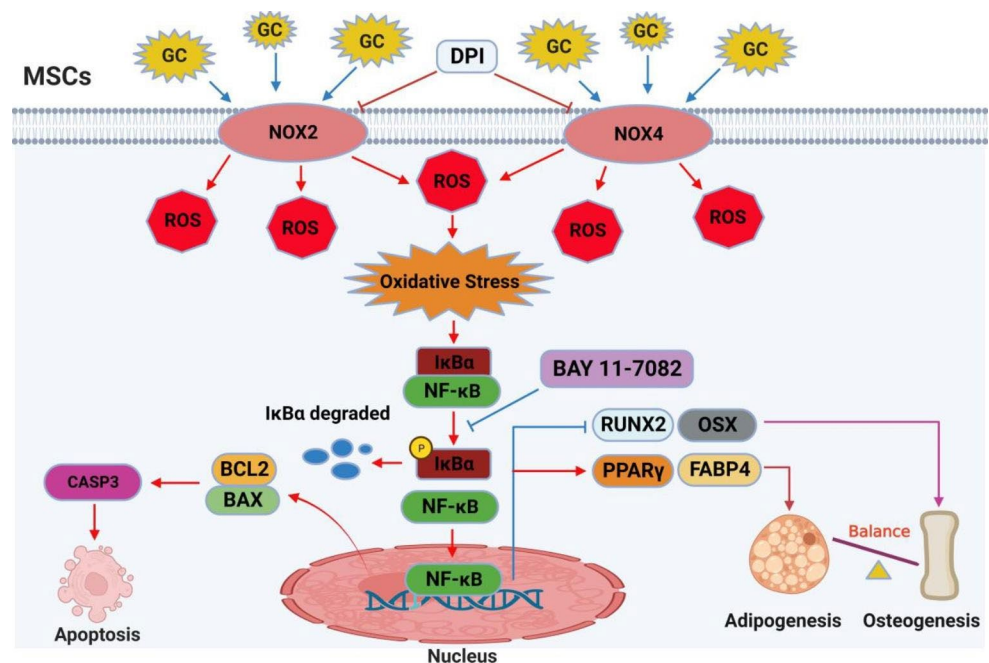
Discussion

The pathogenesis of GONFH has yet to be elucidated. Therefore, a proper animal model is essential to study the molecular and cellular mechanisms of GONFH. The rat is considered a cost-effective animal model to establish GONFH; however, no standard induction protocol has been well established. Currently, there are three main methods used to establish rat GONFH models. MPS alone, [31] MPS combined with allogeneic serum, [32] and LPS combined with MPS [33]. In the present study, histopathological and radiological comparisons revealed that the LPS in combination with the MPS model was extremely similar to that of patients with early GONFH, as demonstrated by reduced bone mass in the subchondral bone and a marked increase in

the rate of empty bone traps and adipocyte area. Therefore, our rat model of GONFH is an optimal preclinical animal model to date.

Though the pathogenic factors of GONFH remain unclear, exacerbation of the OS microenvironment through excessive elevation of ROS may be a potential factor in pathogenesis [26,34,35]. Physiological levels of GCs are necessary for the proliferation and differentiation of MSCs [36]. Nevertheless, excessive GCs increase ROS levels in MSCs, osteoblasts, osteocytes, etc., [4,10] thereby exacerbating the intracellular OS microenvironment. Evidence suggests extensive inflammatory cell infiltration occurs after femoral head necrosis, resulting in excessive ROS production in MSCs, ultimately exacerbating the GONFH process [37]. In agreement with their findings, our data indicated that high doses of GCs increased ROS levels *in vivo* and *in vitro*. Moreover, it was shown that the fate of MSCs is a crucial factor in determining the GONFH progression. The NOX family plays a pivotal role in oxidant responses and is a major source of ROS in bone and cells, with NOX2 and NOX4 proteins being the most prominent [28–30]. Moreover, at high concentrations, GCs induced apoptosis [8] and an imbalance in osteogenic/lipogenic differentiation of MSCs [7]. Furthermore, based on the enormous role played by the OS microenvironment in cell apoptosis and differentiation, it is plausible to hypothesize that excessive GCs lead to apoptosis and an imbalance in osteogenic/lipogenic differentiation of MSCs by increasing NOX protein expression and thus elevate intracellular ROS levels. Amazingly, the DEX-induced apoptosis and destabilization of osteogenic/lipogenic differentiation of MSCs were significantly reversed when co-treated with the NOX inhibitor.

Fig. 7 Schematic diagram of the pathogenesis of GONFH. The exacerbation of the OS microenvironment in MSCs induced by high doses of GCs leading to apoptosis and differentiation imbalance is a pivotal factor in the pathogenesis of GONFH, mediated by activation of the NOX/ROS/NF- κ B signaling pathway



Thus, OS-induced apoptosis and imbalance in osteogenic/lipogenic differentiation of MSCs may be critical contributing factors to GONFH. Inhibition of ROS produced by NOX family proteins has a potential therapeutic effect on GONFH.

NF- κ B performs a pivotal role in inflammation, cell proliferation, cell differentiation and apoptosis [17–19]. In addition, NF- κ B is an important redox-sensitive transcription factor whose activity can be directly augmented or repressed by ROS in a context-dependent manner [38,39]. NF- κ B is a critical downstream target of ROS in various processes such as inflammatory response, cytotoxicity, and survival and invasion of cancer cells [40,41]. Meanwhile, it has been shown that elevated ROS levels can specifically activate NF- κ B [42]. Therefore, we hypothesized that excessive activation of the NOX/ROS/NF- κ B signaling pathway might be implicated in the pathogenesis of GONFH. Moreover, recent researches have confirmed that activation of NF- κ B affects apoptosis and differentiation of MSCs [43,44]. Surprisingly, our results showed that apoptosis and differentiation imbalance induced by high doses of GCs in MSCs was significantly reversed using BAY 11-7082. However, NF- κ B has been shown to regulate redox homeostasis. NF- κ B might regulate ROS levels by modulating ROS production and antioxidant enzymes [45,46]. Interestingly, our *in vitro* results indicated that the NF- κ B inhibitor-BAY 11-7082 failed to prevent the production of ROS and elevated NOX2 and NOX4 gene expression due to excess GCs, which further supported that ROS production upstream of NF- κ B [40,41], at least in MSCs. As shown in Fig. 7, our study revealed that GCs lead to apoptosis and imbalance in osteogenic/lipogenic differentiation of MSCs through activation of NOX/ROS/NF- κ B signaling.

Inevitably, this study has some limitations. There is no universally accepted animal model of GONFH. Although our animal model is similar to the pathological features of early GONFH patients, we could not observe the pathological alterations and mechanisms of the whole GONFH process. Future studies may extend the moulding time and improve the moulding method to mimic the pathological features of GONFH patients better. In addition, our results did not exclude the involvement of signaling pathways other than NOX/ROS/NF- κ B in the development of GONFH. Therefore, other meaningful signaling pathways deserve further investigation.

Conclusion

Together, we proved for the first time that the exacerbation of the OS microenvironment in MSCs induced by high doses of GCs leading to apoptosis and differentiation imbalance

is indeed a pivotal factor in the pathogenesis of GONFH, mediated through activating the NOX/ROS/NF- κ B signaling pathway. The current study suggested that inhibition of ROS levels and NF- κ B activity may be an emerging strategy to prevent and treat GONFH.

Author contributions The authors confirm contribution to the paper as follows: study conception and design: Luwei Xiao, Peijian Tong, Hongting Jin; Experiment and data collection: Huihui Xu, Qinghe Zeng, Kaiao Zou, Haipeng Huang, Jiali Chen; Analysis and interpretation of results: Huihui Xu, Qinghe Zeng, Kaiao Zou, Pinger Wang, Wenhua Yuan; Draft manuscript preparation: Huihui Xu, Qinghe Zeng, Kaiao Zou. All authors reviewed the results and approved the final version of the manuscript.

Funding This work has been partially supported by the Natural Science Foundation of China (Grant No. 81873325), and the State Administration of Traditional Chinese Medicine of Zhejiang Province (Grant No. 2021ZZ014).

Data Availability Data can be available upon request from the corresponding author.

Declarations

Ethical approval The study was approved by the Ethics Committee of the First Affiliated Hospital of Zhejiang Chinese Medical University (No. 2018-KL-005-02). All animal experiments in the present study were permitted by the Ethics Committee of Zhejiang Chinese Medical University (No. 20190401-10) and conducted according to the NIH Guide for the Care and Use of Laboratory Animals.

Consent for publication All authors consent to submit the manuscript for publication.

Competing interests The authors declare that they have no competing of interest.

References

1. Lu C, Qi H, Xu H et al (2022) Global research trends of steroid-induced osteonecrosis of the femoral head: a 30-year bibliometric analysis. *Front Endocrinol (Lausanne)* 13:1027603
2. Agarwal A, Rochwerger B, Lamontagne F et al (2020) A living WHO guideline on drugs for covid-19. *BMJ* 370:m3379
3. Guo KJ, Zhao FC, Guo Y, Li FL, Zhu L, Zheng W (2014) The influence of age, gender and treatment with steroids on the incidence of osteonecrosis of the femoral head during the management of severe acute respiratory syndrome: a retrospective study. *Bone Joint J* 96-B(2):259–262
4. Yang N, Sun H, Xue Y et al (2021) Inhibition of MAGL activates the Keap1/Nrf2 pathway to attenuate glucocorticoid-induced osteonecrosis of the femoral head. *Clin Transl Med* 11(6):e447
5. Zhou M, Xi J, Cheng Y et al (2021) Reprogrammed mesenchymal stem cells derived from iPSCs promote bone repair in steroid-associated osteonecrosis of the femoral head. *Stem Cell Res Ther* 12(1):175
6. Wu X, Sun W, Tan M (2019) Noncoding RNAs in Steroid-Induced osteonecrosis of the femoral head. *Biomed Res Int* 2019:8140595

7. Wang G, Wang F, Zhang L, Yan C, Zhang Y (2021) miR-133a silencing rescues glucocorticoid-induced bone loss by regulating the MAPK/ERK signaling pathway. *Stem Cell Res Ther* 12(1):215
8. Wang Y, Luan S, Yuan Z et al (2022) The combined use of platelet-rich plasma clot releasate and Allogeneic Human umbilical cord mesenchymal stem cells rescue Glucocorticoid-Induced osteonecrosis of the femoral head. *Stem Cells Int* 2022:7432665
9. Li J, Zhang N, Huang X et al (2013) Dexamethasone shifts bone marrow stromal cells from osteoblasts to adipocytes by C/EBP α promoter methylation. *Cell Death Dis* 4(10):e832
10. Chen L, Hu SL, Xie J et al (2020) Proanthocyanidins-mediated Nrf2 activation ameliorates Glucocorticoid-Induced oxidative stress and mitochondrial dysfunction in osteoblasts. *Oxid Med Cell Longev* 2020:9102012
11. Mo Y, Lai W, Zhong Y et al (2021) TXNIP contributes to bone loss via promoting the mitochondrial oxidative phosphorylation during glucocorticoid-induced osteoporosis. *Life Sci* 266:118938
12. Rai D, Tripathi AK, Sardar A et al (2022) A novel BMP2 secretagogue ameliorates glucocorticoid induced oxidative stress in osteoblasts by activating NRF2 dependent survival while promoting Wnt/ β -catenin mediated osteogenesis. *Free Radic Biol Med* 190:124–147
13. Ben Othmene Y, Monceaux K, Belhadef A et al (2022) Triazole fungicide tebuconazole induces apoptosis through ROS-mediated endoplasmic reticulum stress pathway. *Environ Toxicol Pharmacol* 94:103919
14. Zhou X, Zhang X, Wu Z et al (2021) The novel ALK inhibitor ZX-29 induces apoptosis through inhibiting ALK and inducing ROS-mediated endoplasmic reticulum stress in Karpas299 cells. *J Biochem Mol Toxicol* 35(3):e22666
15. Zhu YL, Huang J, Chen XY et al (2022) Senkyunolide I alleviates renal ischemia-reperfusion injury by inhibiting oxidative stress, endoplasmic reticulum stress and apoptosis. *Int Immunopharmacol* 102:108393
16. Atashi F, Modarressi A, Pepper MS (2015) The role of reactive oxygen species in mesenchymal stem cell adipogenic and osteogenic differentiation: a review. *Stem Cells Dev* 24(10):1150–1163
17. Hoesel B, Schmid JA (2013) The complexity of NF- κ B signaling in inflammation and cancer. *Mol Cancer* 12:86
18. Yildirim E, Sezer G (2021) Clinical plasma concentration of vinpocetine does not affect osteogenic differentiation of mesenchymal stem cells. *Pharmacol Rep* 73(1):202–210
19. Constanze B, Popper B, Aggarwal BB, Shakibaei M (2020) Evidence that TNF- β suppresses osteoblast differentiation of mesenchymal stem cells and resveratrol reverses it through modulation of NF- κ B, Sirt1 and Runx2. *Cell Tissue Res* 381(1):83–98
20. Zhu W, Guo M, Yang W et al (2020) CD41-deficient exosomes from non-traumatic femoral head necrosis tissues impair osteogenic differentiation and migration of mesenchymal stem cells. *Cell Death Dis* 11(4):293
21. Yin X, Zhang J, Zhao W, Liu Z, Wang J (2022) Combined Levotetrahedralpalmitine and diphenyleneiodonium chloride enhances antitumor activity in hepatocellular carcinoma. *Pharmacol Res* 179:106219
22. Ge Q, Ying J, Shi Z et al (2021) Chlorogenic acid retards cartilaginous endplate degeneration and ameliorates intervertebral disc degeneration via suppressing NF- κ B signaling. *Life Sci* 274:119324
23. Jiang HT, Ran CC, Liao YP et al (2019) IGF-1 reverses the osteogenic inhibitory effect of dexamethasone on BMP9-induced osteogenic differentiation in mouse embryonic fibroblasts via PI3K/AKT/COX-2 pathway. *J Steroid Biochem Mol Biol* 191:105363
24. Xu H, Fang L, Zeng Q et al (2022) Glycyrrhizic acid alters the hyperoxidative stress-induced differentiation commitment of MSCs by activating the Wnt/ β -catenin pathway to prevent SONFH. *Food Funct*
25. Xu HH, Li SM, Fang L et al (2021) Platelet-rich plasma promotes bone formation, restrains adipogenesis and accelerates vascularization to relieve steroids-induced osteonecrosis of the femoral head. *Platelets* 32(7):950–959
26. Chen K, Liu Y, He J et al (2020) Steroid-induced osteonecrosis of the femoral head reveals enhanced reactive oxygen species and hyperactive osteoclasts. *Int J Biol Sci* 16(11):1888–1900
27. Chen J, Cui Z, Wang Y et al (2022) Cyclic polypeptide D7 protects bone marrow mesenchymal cells and promotes chondrogenesis during osteonecrosis of the femoral head via growth differentiation factor 15-Mediated Redox Signaling. *Oxid Med Cell Longev* 2022:3182368
28. Werner SL, Sharma R, Woodruff K et al (2020) CSF-1 in Osteocytes inhibits Nox4-mediated oxidative stress and promotes normal bone homeostasis. *JBM Plus* 4(7):e10080
29. Brandes RP, Weissmann N, Schroder K (2014) Nox family NADPH oxidases: molecular mechanisms of activation. *Free Radic Biol Med* 76:208–226
30. Brewer TF, Garcia FJ, Onak CS, Carroll KS, Chang CJ (2015) Chemical approaches to discovery and study of sources and targets of hydrogen peroxide redox signaling through NADPH oxidase proteins. *Annu Rev Biochem* 84:765–790
31. Zhang Y, Yin J, Ding H, Zhang C, Gao YS (2016) Vitamin K2 ameliorates damage of blood vessels by glucocorticoid: a potential mechanism for its Protective Effects in glucocorticoid-induced osteonecrosis of the femoral head in a rat model. *Int J Biol Sci* 12(7):776–785
32. Wang L, Luo DK, Pan ZY (2013) Expression of 11 β -HSD in steroid-induced avascular necrosis of the femoral head. *Mol Med Rep* 7(5):1482–1486
33. Zheng LZ, Wang JL, Kong L et al (2018) Steroid-associated osteonecrosis animal model in rats. *J Orthop Translat* 13:13–24
34. Deng G, Niu K, Zhou F et al (2017) Treatment of steroid-induced osteonecrosis of the femoral head using porous Se@SiO₂ nanocomposites to suppress reactive oxygen species. *Sci Rep* 7:43914
35. Zhang F, Yan Y, Peng W et al (2021) PARK7 promotes repair in early steroid-induced osteonecrosis of the femoral head by enhancing resistance to stress-induced apoptosis in bone marrow mesenchymal stem cells via regulation of the Nrf2 signaling pathway. *Cell Death Dis* 12(10):940
36. Smith KA, Waypa GB, Schumacker PT (2017) Redox signaling during hypoxia in mammalian cells. *Redox Biol* 13:228–234
37. Sung YJ, Kao TY, Kuo CL et al (2018) Mitochondrial lon sequestrers and stabilizes p53 in the matrix to restrain apoptosis under oxidative stress via its chaperone activity. *Cell Death Dis* 9(6):697
38. Loukili N, Rosenblatt-Velin N, Rolli J et al (2010) Oxidants positively or negatively regulate nuclear factor κ B in a context-dependent manner. *J Biol Chem* 285(21):15746–15752
39. Rajendrasozhan S, Yang SR, Edirisinghe I, Yao H, Adenuga D, Rahman I (2008) Deacetylases and NF- κ B in redox regulation of cigarette smoke-induced lung inflammation: epigenetics in pathogenesis of COPD. *Antioxid Redox Signal* 10(4):799–811
40. Zhang X, Liu J, Pang X, Zhao J, Wang S, Wu D (2014) Aldosterone induces C-reactive protein expression via MR-ROS-MAPK-NF- κ B signal pathway in rat vascular smooth muscle cells. *Mol Cell Endocrinol* 395(1–2):61–68
41. Jin X, Song L, Liu X et al (2014) Protective efficacy of vitamins C and E on p,p'-DDT-induced cytotoxicity via the ROS-mediated mitochondrial pathway and NF- κ B/FasL pathway. *PLoS ONE* 9(12):e113257
42. Bouyahya A, El Menyiy N, Oumeslakht L et al (2021) Preclinical and clinical antioxidant Effects of Natural Compounds against

- oxidative Stress-Induced Epigenetic instability in Tumor cells. *Antioxid (Basel)* ;10(10)
43. Sonowal H, Ramana KV (2020) 2'-Hydroxyflavanone prevents LPS-induced inflammatory response and cytotoxicity in murine macrophages. *Toxicol In Vitro* 69:104966
 44. Liu L, Zhao L, Liu Y, Yu X, Qiao X (2022) Rutin ameliorates Cadmium-Induced necroptosis in the Chicken liver via inhibiting oxidative stress and MAPK/NF-kappaB pathway. *Biol Trace Elem Res* 200(4):1799–1810
 45. Morgan MJ, Liu ZG (2011) Crosstalk of reactive oxygen species and NF-kappaB signaling. *Cell Res* 21(1):103–115
 46. George LE, Lokhandwala MF, Asghar M (2012) Novel role of NF-kappaB-p65 in antioxidant homeostasis in human kidney-2 cells. *Am J Physiol Renal Physiol* 302(11):F1440–1446

Publisher's Note Springer Nature remains neutral with regard to jurisdictional claims in published maps and institutional affiliations.

Springer Nature or its licensor (e.g. a society or other partner) holds exclusive rights to this article under a publishing agreement with the author(s) or other rightsholder(s); author self-archiving of the accepted manuscript version of this article is solely governed by the terms of such publishing agreement and applicable law.